750 V Si/SiC Fusion Switches for Automotive Traction Inverters: A Study on the Effects of Reduced SiC MOSFET Die Areas within a Vehicle Application of the Stellantis Group

Tomas Reiter [1], Martin Gleich [1], Franck Briault [2]

[1] Infineon Technologies AG, Neubiberg, Germany
[2] Stellantis, Carrières-sous-Poissy, France

Abstract: Increasing the efficiency of automotive traction inverters while keeping initial costs low has always been a key objective. This contribution studies the potential of Si/SiC-based inverters for peak power ratings ranging from 80 to 150 kW, with the aim of addressing a specific B to C vehicle segment application within the Stellantis Group. Power module configurations with different IGBT/SiC MOSFET die area share rates, as well as different SiC MOSFET areas, will be compared using a bias-aware delta-simulation approach for the inverter within the vehicle simulation. The discussion is supported by experimental testing of the inverters. Finally, the benefits of drive cycle improvements will be translated into battery savings, and the resulting sweet spot of Si/SiC Fusion switch power modules will be evaluated under various vehicle and drive cycle scenarios.

Keywords: Automotive; Traction Inverter; Si/SiC Fusion switch; IGBT; SiC MOSFET; bias-aware delta-simulation; Drive Cycle Efficiency

1 Introduction

Increasing the efficiency of automotive traction inverters while keeping initial costs low has always been a key objective. The implementation of wide bandgap silicon carbide MOSFETs in recent years has brought significant efficiency gains [1]–[4]. Additionally, optimized manufacturing processes have led to a substantial reduction in die cost. However, according to recent benchmarking studies [5], [6], the die cost per area for SiC MOSFETs is still 8 to 12 times higher than for silicon IGBT/Diodes. While a significant portion of this higher cost is compensated by the increased power density of SiC MOSFETs, resulting in reduced power losses and a lower needed battery capacity, which in turn reduces system costs. It is due to the fact that these car types have a high battery capacity to ensure a long electric vehicle driving range autonomy, provide fast charging options through an 850 V power net architecture, and the power modules for the inverters are designed for high output power, thus requiring low-ohmic MOSFETs. The clear result is that the higher die cost of the SiC MOSFETs is easily compensated by the battery cost savings.

However, for the high-volume B and C car segment in the entry class, it is not yet clear. On one hand, the vehicle voltage class for this segment still remain at 470 V, which is less favorable for SiC MOSFETs. While [2] reports an EV range gain of 3.1% to 7.3% in highway to the EPA drive cycles when transitioning from IGBT to SiC MOSFETs at a 1200 V blocking rating in an 800 V supply architecture, a separate study [3] found a significant lower gain of 0.66% to 3.1% in highway to WLTP drive cycles at 450 V working voltage with 750 V blocking rating IGBT and SiC MOSFET devices. Another important consideration for the B and C vehicle segments is the significantly smaller battery sizes with lower maximum allowed charge rates and cost per kWh, which makes cost compensation in these systems more challenging. And last but not least, while a high inverter output performance is desired to achieve good acceleration power, it is a less important feature for this kind of car segment.

With the introduction of the Si/SiC Fusion switch configuration, which offers the advantage of single gate drive capability without requiring changes to software and gate driver architectures, an additional option for inverter design is provided [7], [8]. In [9], [10], Si/SiC Fusion switches for 200 kW peak power-rated inverters have demonstrated an electric drive range gain of 3 to 6% compared to benchmark IGBT inverters, despite containing only

30 to 40% of the SiC MOSFET chip content compared to full SiC MOSFET-based inverters. In [11], it was shown that the SiC die areas in Si/SiC Fusion power modules can be easily scaled while maintaining the single gate drive feature. Additionally, lifetime degradation testing was performed, including repetitive short-circuit testing up to 1 million short-circuit pulses, and no visible electric device degradation was observed, demonstrating the high robustness of this Si/SiC approach.

The impact of different SiC die areas on the vehicle drive range and inverter energy loss over different vehicle types and mission profiles has not yet been investigated and will be the subject of this contribution.

The paper is structured as follows. Section 2 provides an overview of the different vehicle types, mission profiles, motors, and power module configurations (DUTs) investigated within this paper. Section 3 introduces a bias-aware simulation method that uses measured inverter power loss and a delta-simulation approach suited for accurate energy loss prediction over drive cycle profiles. Section 4 compares the measured inverter power losses of the DUTs. Section 5 discusses the energy efficiency of the different power module configurations within the vehicle system simulation, followed by a conclusion.

2 Vehicle Types, Mission Profiles, Motor, and Power Module Configuration

Within the studies, one of the targets was to analyze how different vehicle types (i.e., different masses and body styles) within the B and C car segment, as well as the driving profile referred to as the mission profile, will influence the selection of IGBT, Si/SiC, and SiC modules with respect to energy efficiency. An overview of the vehicles are listed in Table 1. The vehicle was modeled using a behavioral model with simplified linear longitudinal dynamics, including the vehicle mass, aerodynamic resistance, rolling resistance, wheel size, and gear ratio.

The permanent magnet synchronous motor (PMSM) was modeled via fine-grained lookup tables filled from a finite element simulation. The used motor phase current map versus speed/torque is shown in Fig. 2 as an example.

An overview of the different power module configurations within this comparison is provided in Table 3. All chipsets are from an automotive-released 750 V technology. The IGBTs are micropattern trench EDT3, and the SiC devices are from automotive 2nd generation trench MOSFETs. All parts were tested in same power module package with direct fluid cooling via PinFin structure.

In summary, from the vehicle simulation model, a speed-torque command was created. The motor lookup table provides the motor power losses and the required inverter phase voltage and currents, including the resulting power factor, which are the inputs for the inverter power loss simulations discussed in detail in Section 3.

The simplifications in the vehicle and motor mod-

Tab. 1: Vehicle Types for Simulation Model

Vehicle Name	MINI	AVERAGE	MAXI
Mass [t]	1.6	1.8	2.1
Body Style	Hatchback	B-SUV	Sedan
Battery Voltage	280..470 V		
Inverter Current Ampacity	450..650 Arms		

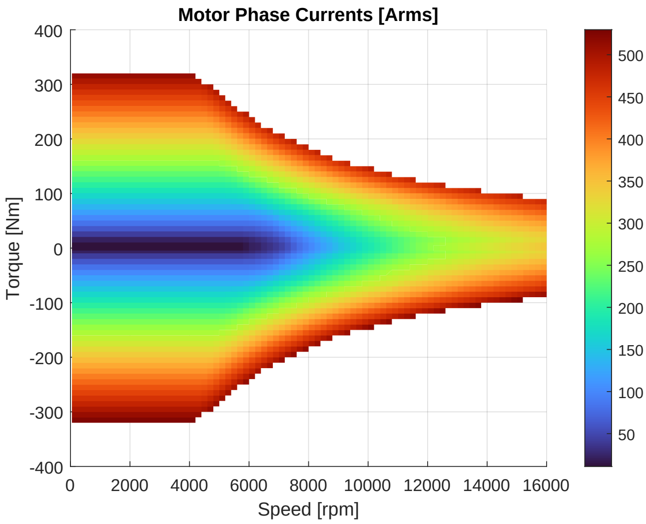

Tab. 2: PMSM 150 kW Motor lookup table used for all vehicle types.

Tab. 3: Power Module Configurations

Part	Si Area [mm²]	SiC Area [mm²]	Ampacity [Arms][1]	rel Die Cost [%][2]
IGBT	320/180	0	800	100
FU3	160/60	60	750	200
FU2	160/60	40	680	150
FU1	160/60	20	590	100
SiC 8	0	160	700	400
SiC 6	0	120	500	300
SiC 4	0	80	400	200

[1] current ampacity acc. to [11].
[2] rounded to 50% and cost input acc. to [5], [6].

els can be justified here, as the main motivation was to understand the influence between different vehicles rather than making absolute drive cycle energy consumption conclusions about a specific car model. In contrast, the inverter simulation requires high accuracy in order to make an assessment of the suitable use of different power modules possible.

3 Bias-aware Delta-Simulation Method

In theory, the ideal solution for comparing different power modules in vehicles and mission profiles would be to measure them all on an inverter motor test bench. However, with all the combinations, the test time needs to be reduced while maintaining high accuracy. A special challenge are the inverter light load conditions, which occur frequently within the drive cycles. In studies like [12], more detailed inverter simulation models using 2nd order polynomial functions were proposed. However, even under such simulation approaches, a high discrepancy compared to real testing can occur due to the neglect of several real effects, as summarized below.

- Only the main part of the switching energy is included (see Fig. 1).
- Capacitive related power losses are ignored completely (see Fig. 4, zoom at I_{ph} = 0 Arms).
- Diode turn-on (forw. recovery) is ignored [4].
- Body diode conduction during PWM dead time is ignored [4].
- Synchronous rectification turn-on and turn-off are assumed to be ideal, with zero losses [4].

These power loss contributions can often be ignored for designing the inverter application at nominal load conditions, but can contribute significantly in the drive cycle's relevant light load area, as discussed in [4], where just the PWM dead time-related power losses alone accounted for about 10 to 15% of the total inverter power losses.

The influence of applying different integral limits is often overlooked. While the IEC 60747-9:2019 standard for IGBT defines the integral limits from 10% V_{gs} to 2% V_{ds} at turn-on to be applied, the MOSFET-related standard IEC 60747-8:2010 defines it different with 10% I_d to 10% V_{ds} removing by nomenclature already a certain amount of real switching losses for the datasheet specifications. To illustrate the influence of different integral limits,

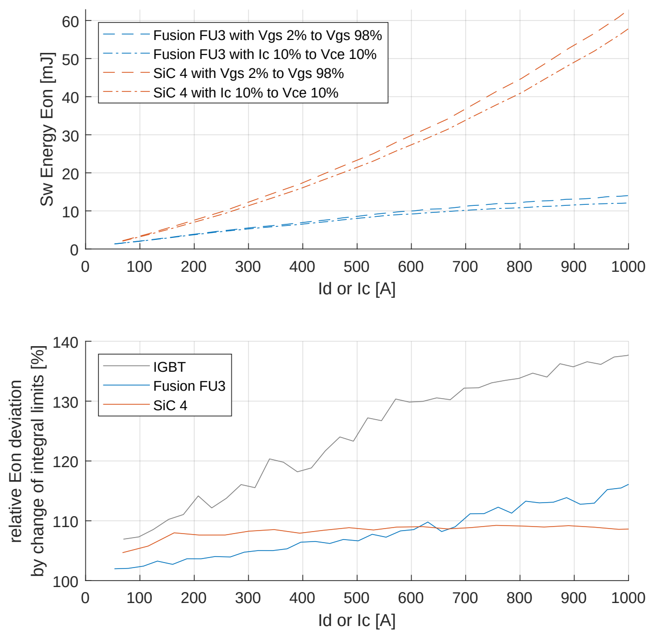

Fig. 1: Influence of the extracted switching losses of device double pulse characterization with different switching energy per pulse integral limits.

Figure 1 shows the extracted turn-on switching energies per pulse, as well as the relative deviation when changing the limits, from the widest practical applicable limit (2% V_{gs} to 98% V_{gs}) to the MOSFET applied narrow limit (10% I_d to 10% V_{ds}). The influence is often in the range of 10%, but importantly, the shape of the switching curve itself will significantly impact the effect of different nomenclatures. As seen in the plot, this results in no constant offset, highlighting the complexity of the relationship between integral limits and switching energy extraction. The discussed integral limits at the turn-on energies (Eon) apply with the same principles also to the turn-off (Eoff) and diode turn-off (Erec). However, it is quite obvious that changing the methodology for switching energy extraction will not change the actual resulting power losses in an application.

To address this challenge, a bias-aware simulation approach was selected. The method itself is derived from global climate modeling, where local temperature deviations were observed to be nearly constant. Climate predictions of the past, together with local measurements, can correct local predictions in the climate model [13]. This basic principle was then transferred to inverter power loss simulation.

Each inverter was measured over a reduced operating parameter set ($\mathrm{OP_{meas}}$) by characterizing its input-to-output power losses ($\mathrm{P_{loss,meas}}$) and stor-

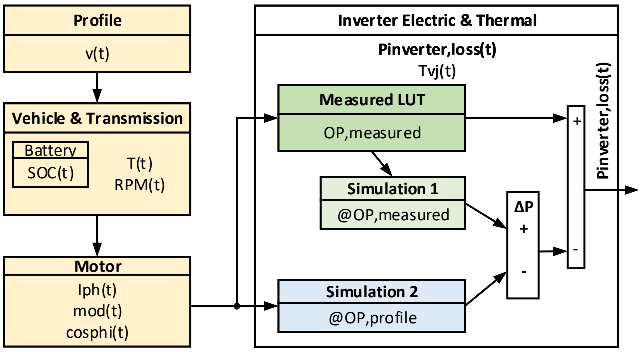

Fig. 2: Illustration of the bias-aware delta-simulation method of the traction inverter for drive cycle simulation.

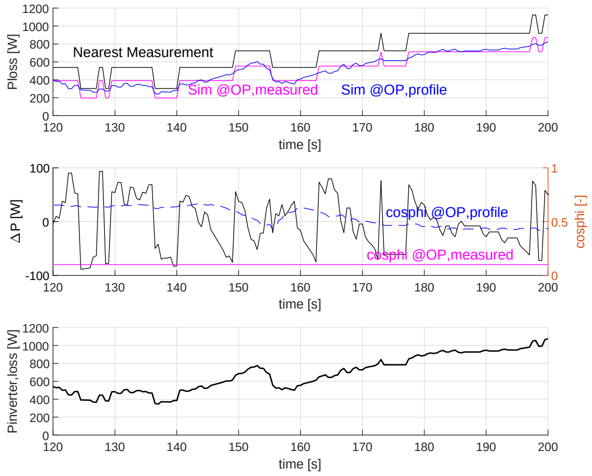

Fig. 3: Example of the bias-aware delta-simulation. For method explanation the this example show a reduced dataset of the measurements.

ing the data in a lookup table. The measured data set is shown in Fig. 4. Within the mission profile simulation, this lookup table was combined with a delta-simulation approach. The first inverter power loss simulation is performed at the nearest operating point provided in the lookup table ($\mathrm{OP_{meas}}$), and the second simulation is performed at the operating condition required for the actual mission profile point (see also Equations 1 and 2).

$$\mathrm{P_{inverter,loss}} = \mathrm{P_{loss,meas}}\left(\mathrm{OP_{meas}}\right) - \Delta\mathrm{P} \quad (1)$$

$$\Delta\mathrm{P} = \mathrm{P_{loss,sim}}\left(\mathrm{OP_{meas}}\right) - \mathrm{P_{loss,sim}}\left(\mathrm{OP_{profile}}\right) \quad (2)$$

An illustration of the bias-aware delta-simulation method is shown in Fig. 2. This approach includes all power losses that occur in reality, while keeping the measurement effort at a low level.

An example of the method is further illustrated in Fig. 3, where the measured dataset has been reduced to facilitate explanation. The nearest measurement points exhibit large steps because not all conditions have been measured. However, the simulations of both the measured operating condition and the profile condition show an offset, which does not impact the results since only the delta values are required. Therefore, the primary focus is on the relative accuracy of the simulation models. Additionally, the amplitude of the ΔP values can serve as an indicator for recommending additional measurement points in the future. If the ΔP values are high, introducing an extra measurement point may potentially enhance the accuracy of the system simulation.

The method employed here for power loss simulation can be easily adapted for other applications, such as estimating power cycling lifetime, where high precision in simulating junction temperature is crucial to match real-world conditions.

4 Measured Inverter Power Losses

All power modules listed in Table 3 were tested on an inverter test bench. A detailed documentation of the lab equipment and measurement settings used can be found in [4].

Implementing parallel SiC die content alongside the IGBT can cut down power losses, especially at low currents, by a factor of two, depending on the amount of SiC area implemented. For a more holistic comparison, the line colors were selected to correlate with the implemented die cost within the power module configurations. Below 25 Arms, the best option among the Si/SiC Fusion configurations was the one where only a single SiC die of 20 mm^2 was implemented (i.e., a Si/SiC ratio of 11:1). At higher currents, the more SiC MOSFET area implemented, the lower the inverter power losses.

The same procedure was applied to power modules fully populated with SiC MOSFETs. At a load current of 25 Arms, all three tested versions exhibited nearly equal power losses. At around 300 Arms, it becomes clear that a larger SiC MOSFET die area reduces inverter power losses, but also increases the die cost within the parts. An interesting effect was observed at high currents above 500 Arms, where a larger SiC MOSFET chip area did not result in lower inverter power losses. This was attributed to the fact that the paralleled dies, with their reverse recovery behavior, reached overvoltage limitations earlier and thus had to be switched slightly slower. Nevertheless, with a larger total die area, more power can be dissipated, resulting in a higher current ampacity of the power

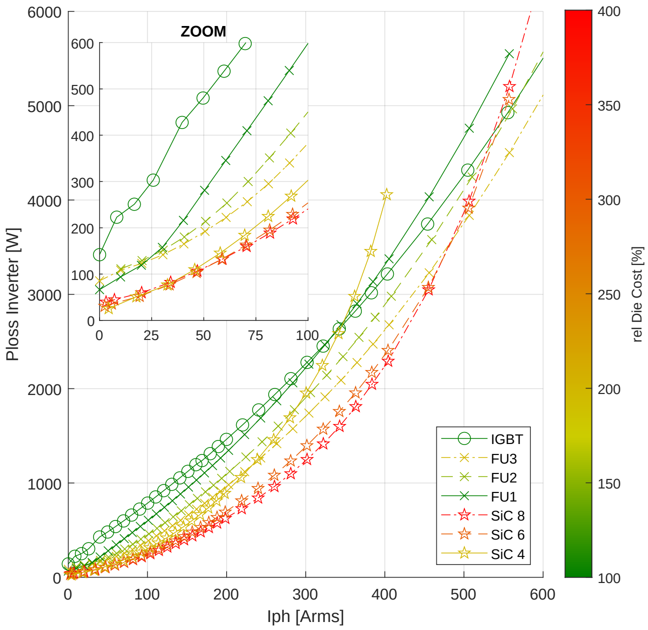

Fig. 4: Measured inverter power losses at a constant working voltage of 450 Vdc, a switching frequency of 10 kHz in space vector modulation, an electric output frequency of 100 Hz, and a coolant inlet temperature of 65 °C at a flow rate of 10 L/min. The line colors represent the relative die cost within the power module DUTs.

module, even if the efficiency itself is no longer increasing at the high currents. Nevertheless, these results clearly demonstrate that measurements on small die areas and heavy upscaling in simulations to larger die areas lead to very non-linear behavior and should be avoided where possible to prevent wrong conclusions.

5 Drive Cycle Efficiency

With the simulation method described earlier, the listed vehicles of Table 1 were equipped with inverter systems of all different power module configurations of Table 3 and simulated under three different mission profiles. The standardized WLTP class 3b and CLTC-P profiles were used as representatives for profiles with a high amount of light load operation. The standardized Artemis-Highway profile, with its 150 km/h top speed as representative for harsher mission profiles, where electric driving range has a high customer value. Fig. 5 shows two examples of vehicle speed and resulting inverter phase currents over time, including a histogram of the phase currents.

Figures 6a to 6i show the results for all variants, where the inverter power losses of each simulation set (,i.e., vehicle and profile) are normalized to the IGBT module with its lowest part cost. The

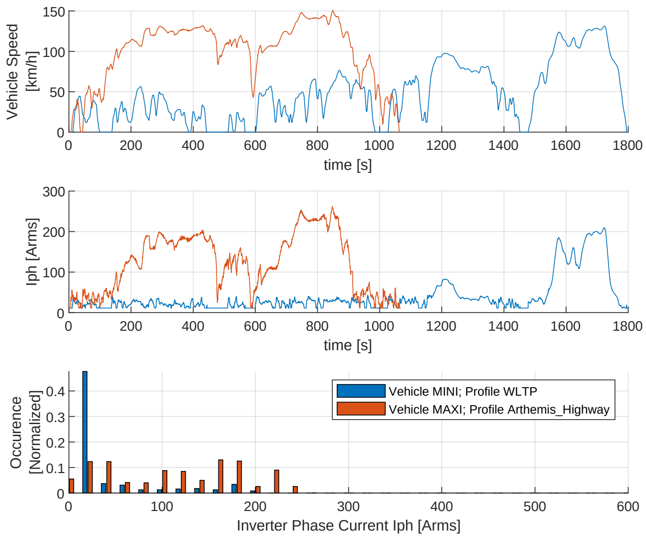

Fig. 5: Mission Profile WLTP and Artemis_Highway, with the resulting inverter phase currents at a 450 V working voltage, in direct comparison.

Tab. 4: Results Vehicle: **MINI**; Profile: **WLTP**

Part	Ampacity Arms	Drive Cycle Cons. kWh/100km (rg[1] %)	Req. Battery >kWh [2]
IGBT	800	14.52 (+0.0%)	n.a.
FU3	750	14.07 (+3.2%)	30
FU2	680	14.11 (+2.9%)	15
FU1	590	14.17 (+2.5%)	5
SIC 8	700	13.89 (+4.5%)	60
SIC 6	500	13.89 (+4.5%)	40
SIC 4	400	13.93 (+4.2%)	25

Tab. 5: Results Vehicle: **MAXI**; Profile: **Arth. Highway**

Part	Ampacity Arms	Drive Cycle Cons. kWh/100km (rg[1] %)	Req. Battery >kWh [2]
IGBT	800	24.89 (+0.0%)	n.a.
FU3	750	24.49 (+1.6%)	55
FU2	680	24.57 (+1.3%)	35
FU1	590	24.72 (+0.7%)	5
SIC 8	700	24.29 (+2.5%)	105
SIC 6	500	24.32 (+2.3%)	75
SIC 4	400	24.43 (+1.9%)	45

[1] rg: relative **r**ange **g**ain to IGBT.
[2] Req. Battery: To compensate additional power module part cost related to IGBT a battery capacity of greater than x kWh will be required. Cost assumption according to [5], [6], [14]. Battery capacity rounded up to 5 kWh segments.

3D bar diagram was selected due to the multidimensional aspect of the data. Changing the die technology and area not only changes the part cost, but also the maximum current ampacity of the power module, making a direct comparison more

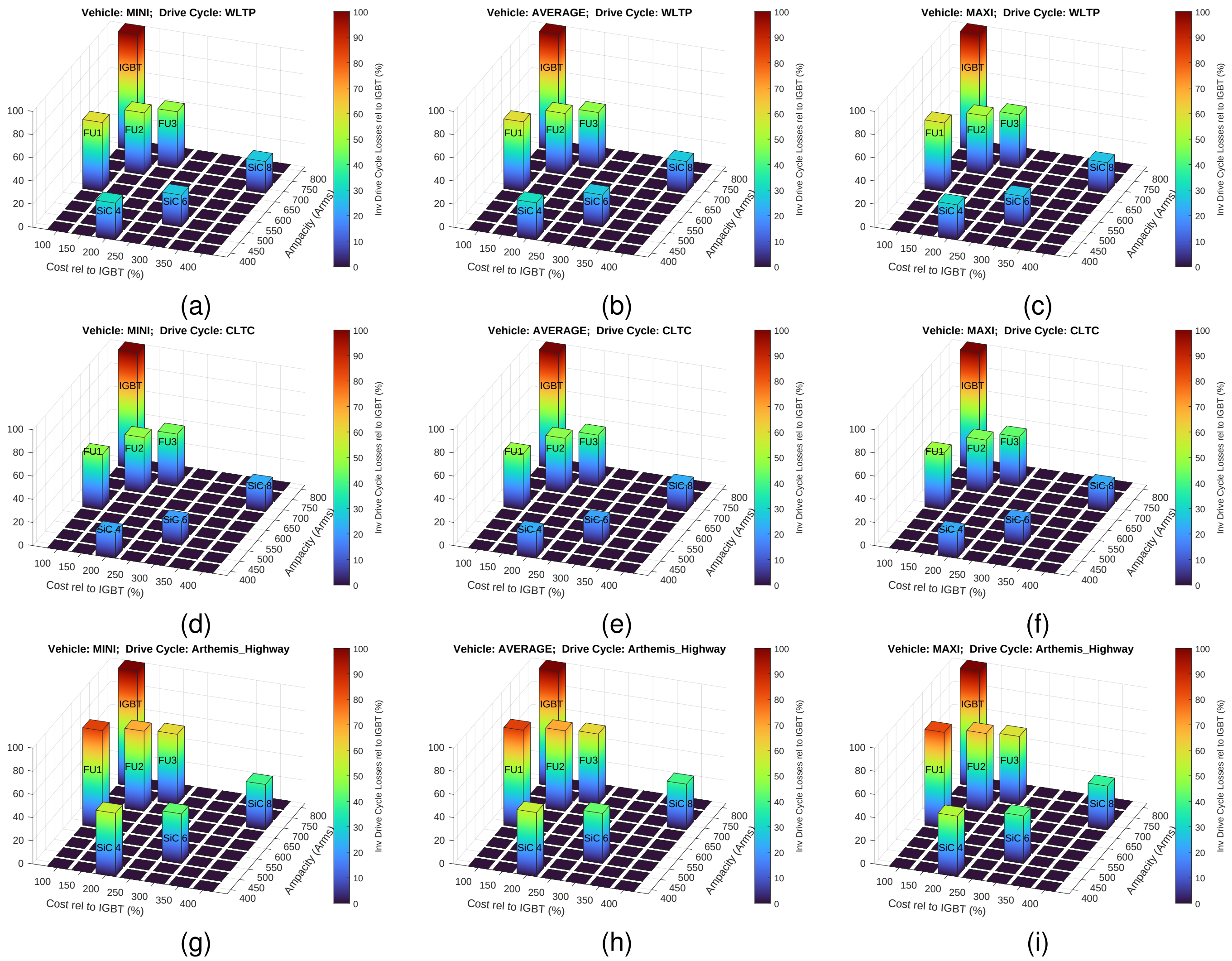

Fig. 6: Inverter drive cycle losses relative to IGBT power module (z-axis) are shown, including relative die cost (x-axis) and power module maximum current ampacity (y-axis), for different vehicles (left to right) and profiles (top to bottom) at 450 V working voltage. The highest die-cost SiC power module configurations result in the lowest losses in all profiles. The Si/SiC Fusion configurations, with a cost close to that of the IGBT configuration, reduce power losses by approximately 50% in WLTP and CLTC, and by 20-45% in highway drive cycles.

complex. However, from these plots, a key finding is that the different vehicle types within the B and C segments can be seen as a minor influence factor for the optimal power module configuration from a drive cycle efficiency perspective (compare the plots from left to right for the different vehicles within the same profile). In contrast, the drive cycle has a much higher impact (compare the plots from top to bottom for the different profiles within the same vehicle). In line with previous studies [2], [3], [9], the SiC MOSFETs as well as the Si/SiC Fusion modules reduce the inverter power losses the most in relaxed drive cycles, but still provide substantial power loss savings in the highway profiles, which will be quantified in more detail in the following discussion.

6 Results Discussion and Switch Technology selection

Already a low amount of SiC MOSFET area within a Si/SiC Fusion configuration, such as the 11:1 share ratio of "FU1", provides a significant loss saving compared to an IGBT module and can be compensated by battery capacity of already 5 kWh, which could make it interesting for entry-class vehicles at first glance. However, the combination of Si and SiC within the power module can hardly be downscaled to a current ampacity of less than 400 A in practice. Therefore, low-cost and simple silicon IGBT/Diode or RC-IGBT power module configurations with low die areas will still lead in this segment.

Within the typical 40 to 75 kW battery sizes of the B and C vehicle segments, the Si/SiC Fusion with die area share rates of "FU2" or "FU3" will pay off due to the resulting higher drive cycle efficiency. When longer EV ranges on highway drive cycles are needed in combination with battery capacities greater than 55 kWh, the FU3 configuration provides the optimal die share ratio.

The full SiC MOSFET solution with the lowest die area (SiC 4) would already compensate for its cost starting from 25 to 45 kWh battery capacity, depending on the drive cycle. However, it does not provide enough current ampacity and thus torque to meet the vehicle design goals. The larger SiC die areas that achieve the required current ampacity start to pay off at battery capacities ranging from 40 to 75 kWh, depending on the drive cycle. The low-ohmic and large-area SiC 8 variant, which can address the entire B and C segment, requires a minimum battery capacity of 60 to 105 kWh for cost compensation. This finding validates again the results from previous studies, conducted several years ago, which showed that SiC MOSFET inverters in the premium segment, with long EV drive ranges and high battery capacities, can easily pay off due to their increased efficiency.

In the segment of B and C vehicles with 40 to 75 kW, the Si/SiC Fusion (FU2 and FU3) provides the best balance between system cost and current ampacity. For inverter systems where the current ampacity is slightly overdimensioned, a reduction of about 20% in current can be achieved by using lower-cost packages, such as low-cost Al2O3 ceramics instead of high-performance Si3N4 ceramics, which can further balance system cost. The smooth switching behavior of Si/SiC Fusion, with its potential to reduce EMI filter efforts [8], [9], its low sensitivity to part-to-part tolerances in terms of current ampacity [11] and [15] gate threshold variations, and its high robustness against short-circuit events [8], [11], [16] can provide additional benefits for further optimization of system cost by implementing Si/SiC Fusion switches in power modules.

Fig. 7 summarizes the resulting choice of switch technologies over a wide area of different vehicle segments, with installed battery capacity on the x-axis and specific battery cost per kWh on the y-axis, resulting from the different required battery charge/discharge rates as well as the needed inverter current ampacity values.

The IGBT remains the choice of solution for the entry class due to its lowest cost and simplicity in

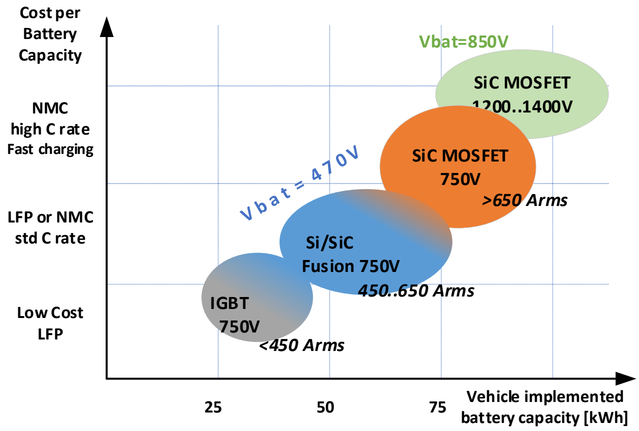

Fig. 7: Resulting switch technology selection.

power module and inverter design. Vehicles with battery capacities beyond 75 kWh are expected to stay with full SiC MOSFET solutions, especially at 850 V working voltage and with fast charging features. In the middle B to C segment, there is room to implement cost/performance-balanced Si/SiC Fusion switch approaches.

The results are expected to be relatively stable over the next 5 to 8 years. Newer SiC MOSFET technologies can certainly increase power density further, but implementation in Si/SiC Fusion can benefit in the same way. Additionally, the further reduction of SiC MOSFET prices on one hand will be offset by further battery cost reductions on the other hand.

7 Conclusion

Several key findings resulted from the studies presented in this paper. 1) Several non-linear effects in power module characteristics are often ignored in simulation models, but can lead to major errors in drive cycle simulations. The introduced bias-aware delta-simulation approach can avoid such errors while keeping measurement efforts low. 2) Different vehicle types within the B and C segments have only a minor influence on the optimal power module configuration from a drive cycle efficiency perspective. 3) For vehicles with battery capacities higher than 75 kWh, inverter systems with full SiC MOSFETs will remain the optimal choice. 4) In the B and C segment, with battery capacities ranging from 40 to 75 kWh, there is room to implement cost/performance-balanced Si/SiC Fusion switch approaches.

References

[1] A. P. Pai, T. Reiter, and M. Maerz, "Efficiency investigation of full-sic versus si-based automotive inverter power modules at equal commutation speed," in *PCIM Europe; International Exhibition and Conference for Power Electronics, Intelligent Motion, Renewable Energy and Energy Management*, 2018. eprint: https://www.researchgate.net/publication/324520965_Efficiency_Investigation_of_Full-SiC_versus_Si-based_Automotive_Inverter_Power_Modules_at_Equal_Commutation_Speed.

[2] A. Allca-Pekarovic, P. J. Kollmeyer, P. Mahvelatishamsabadi, T. Mirfakhrai, P. Naghshtabrizi, and A. Emadi, "Comparison of IGBT and SiC Inverter Loss for 400V and 800V DC Bus Electric Vehicle Drivetrains," in *2020 IEEE Energy Conversion Congress and Exposition (ECCE)*, 2020. DOI: 10.1109/ECCE44975.2020.9236202.

[3] A. Nisch, M. Heller, W. Wondrak, A. Bucher, C. Hasenohr, *et al.*, "Simulation and Measurement-Based Analysis of Efficiency Improvement of SiC MOSFETs in a Series-Production Ready 300 kW / 400 V Automotive Traction Inverter," in *22nd European Conference on Power Electronics and Applications*, 2020. DOI: 10.23919/EPE20ECCEEurope43536.2020.9215765.

[4] T. Reiter, J. Schapdick, M. Krug, M. Muenzer, and F. Wolter, "Pwm dead times in automotive traction inverters using igbt, sic mosfet, or si/sic fusion switch power modules," *IET Power Electronics*, vol. 19, no. 1, e70185, 2026. DOI: https://doi.org/10.1049/pel2.70185.

[5] Yole Group, "Power SiC Transistor Comparison 2025," Yole Group, Tech. Rep. SPR25918, 2025.

[6] ——, "Si IGBT Comparison 2022," Yole Group, Tech. Rep. SPR22646, 2022.

[7] M. Ippisch, T. Reiter, M. Niendorf, W. Jakobi, and M. Muenzer, "Maximizing Cost-Efficiency in Electric Drivetrains: A SiC/Si Fusion Switch Approach," in *PCIM Europe*, 2024. DOI: 10.30420/566262369.

[8] T. Reiter, W. Jakobi, M. Niendor, M. Ippisch, and M. Muenzer, "Fusion switch concept addresses the cost-performance dilemma in EV powertrains," in *PCIM Asia; International Exhibition and Conference for Power Electronics, Intelligent Motion, Renewable Energy and Energy Management*, 2024. DOI: 10.30420/566414053.

[9] T. Reiter and M. Gleich, "Benefits of Si/SiC Fusion Switch for EREV Architectures," in *SIA Powertrain*, Proceedings of SIA Powertrain, 2025. eprint: https://www.researchgate.net/publication/391963871_Benefits_of_SiSiC_Fusion_Switch_for_EREV_Architectures.

[10] H. Baburajan, A. Bucher, C. Hasenohr, A. Rambetius, M. Jahani, and S. Pamarathi, "Practically achievable WLTC loss improvements for the Si/SiC hybrid switch approach in a 400 V automotive traction inverter application – a retrofitting case study," in *PCIM Asia Shanghai Conference 2025; International Exhibition and Conference for Power Electronics, Intelligent Motion, Renewable Energy and Energy Management*, 2025, pp. 487–496. DOI: 10.30420/566583076.

[11] T. Reiter, M. Niendorf, S. Elias, S. D. Pappas, and C. Ouvrard, "Current Ampacity Scaling of Automotive 750 V Si/SiC Fusion Switch and Device Degradation Testing," in *2026 IEEE Applied Power Electronics Conference and Exposition (APEC)*, 2026. eprint: https://www.researchgate.net/publication/402926646_Current_Ampacity_Scaling_of_Automotive_750_V_SiSiC_Fusion_Switch_and_Device_Degradation_Testing.

[12] A. P. Pai, T. Reiter, and M. Maerz, "An improved behavioral model for loss calculations in automotive inverters," in *EEHE - Electric & Electronic Systems in Hybrid and Electrical Vehicles and Electrical Energy Management*, 2016. eprint: https://www.researchgate.net/publication/293334349_An_impoved_behavioral_model_for_loss_calculations_in_automotive_inverters.

[13] C. L. Bruyère, J. M. Done, G. J. Holland, and S. Fredrick, "Bias corrections of global models for regional climate simulations of high-impact weather," *Springer Nature, Climate Dynamics*, vol. 43, pp. 1847–1856, 2014. DOI: https://doi.org/10.1007/s00382-013-2011-6.

[14] D. U. Sauer, "Market observation and technical innovations for lithium-based batteries," in *EEHE - Electric & Electronic Systems in Hybrid and Electrical Vehicles and Electrical Energy Management*, 2025.

[15] M. S. Weidl, F. Wolter, T. Reiter, C. Ouvrard, A. Philippou, *et al.*, "Design Constraints for a Si/SiC Fusion Switch with Realistic Boundary Conditions," in *International Symposium on Power Semiconductor Devices and ICs (ISPSD)*, VDE, 2026. eprint: https://www.researchgate.net/publication/403061727_Design_Constraints_for_a_SiSiC_Fusion_Switch_with_Realistic_Boundary_Conditions.

[16] T. Reiter, J. Schapdick, M. Krug, M. Weinmann, and M. Niendorf, "Active DC-Link capacitor discharge methods with Si/SiC Fusion power module for addressing vehicle cost down," in *PCIM Asia 2025; International Exhibition and Conference for Power Electronics, Intelligent Motion, Renewable Energy and Energy Management*, VDE, 2025. DOI: https://doi.org/10.30420/566583077.